Marine Geology 165 (2000) 27–39

MARINE GEOLOGY
INTERNATIONAL JOURNAL OF MARINE GEOLOGY, GEOCHEMISTRY AND GEOPHYSICS

www.elsevier.nl/locate/margo

Morphodynamics of a large-scale rip current system at Muriwai Beach, New Zealand

R.W. Brander[a,*], A.D. Short[b]

[a]School of Earth Sciences, Victoria University of Wellington, P.O. Box 600, Wellington, New Zealand
[b]Coastal Studies Unit, School of Geosciences, University of Sydney, Sydney, NSW 2006, Australia

Received 6 May 1999; accepted 26 November 1999

Abstract

Field measurements of rip spacing, nearshore morphology, water surface elevation and eulerian and lagrangian flows were made in order to investigate the morphodynamics of a large-scale rip current system at Muriwai Beach, New Zealand. Muriwai is a high-energy meso-tidal beach characterised by modal breaker wave heights of 2.5 m and incident wave periods of 10–15 s. The monitored rip system was characterised by a 400 m long, 75 m wide longshore feeder channel and a 150 m wide rip-neck channel oriented obliquely to the shore and extending over a distance of almost 400 m. During the experiment, the beach evolved from a longshore bar–trough and rip state to a transverse bar and rip configuration. Mean eulerian flow velocities obtained from ducted flowmeters deployed on the *margin* of the feeder channel and rip-neck were on the order of 1 m s^{-1} and instantaneous flows were commonly in excess of 2 m s^{-1}. Mean lagrangian surface flow velocities extending from the base of the feeder through to the rip-head were obtained by tracking rip floaters and were on the order of 0.7 m s^{-1}, with maximums in the rip-neck region of 1.4 m s^{-1}. A distinct tidal modulation of rip current flow existed with maximum velocities occurring at low tide and minimum velocities at high tide. Comparison with other rip studies suggests that although the magnitude of the morphodynamic and hydrodynamic processes occurring within large-scale rip systems is extreme, the behaviour of these rip systems is very similar to low-energy rips with much smaller spatial scales. There is evidence to suggest that distinct morphodynamic scaling relationships exist between these environments.

Keywords: Rip currents; Coastal morphodynamics; High-energy surf zones; New Zealand

1. Introduction

Rip currents are strong, narrow, seaward-flowing currents that begin close to the shore and extend seaward through the surf zone and beyond. They occur on a wide range of beaches, but are particularly common on beaches exhibiting pronounced bar and trough morphology (Wright and Short, 1984; Lippman and Hollman, 1990). Rips often exhibit three interconnected components: (i) longshore feeder currents that convey water into (ii) a narrow rip-neck that flows through the surf zone, eventually decelerating and expanding into (iii) a rip-head seaward of the breakers. This circulation is driven by longshore pressure gradients enhanced by topographic feedback. The feedback mechanism is manifest by more intense wave energy dissipation and set-up occurring across barred areas compared to the rip channels (e.g. Sonu, 1972; Wright et al., 1979; Aagaard et al., 1997). Despite their obvious importance as mechanisms for

* Corresponding author. Fax: +64-4-463-5186.
E-mail addresses: rob.brander@vuw.ac.nz (R.W. Brander), a.short@csu.usyd.edu.au (A.D. Short).

0025-3227/00/$ - see front matter
PII: S0025-3227(00)00004-9

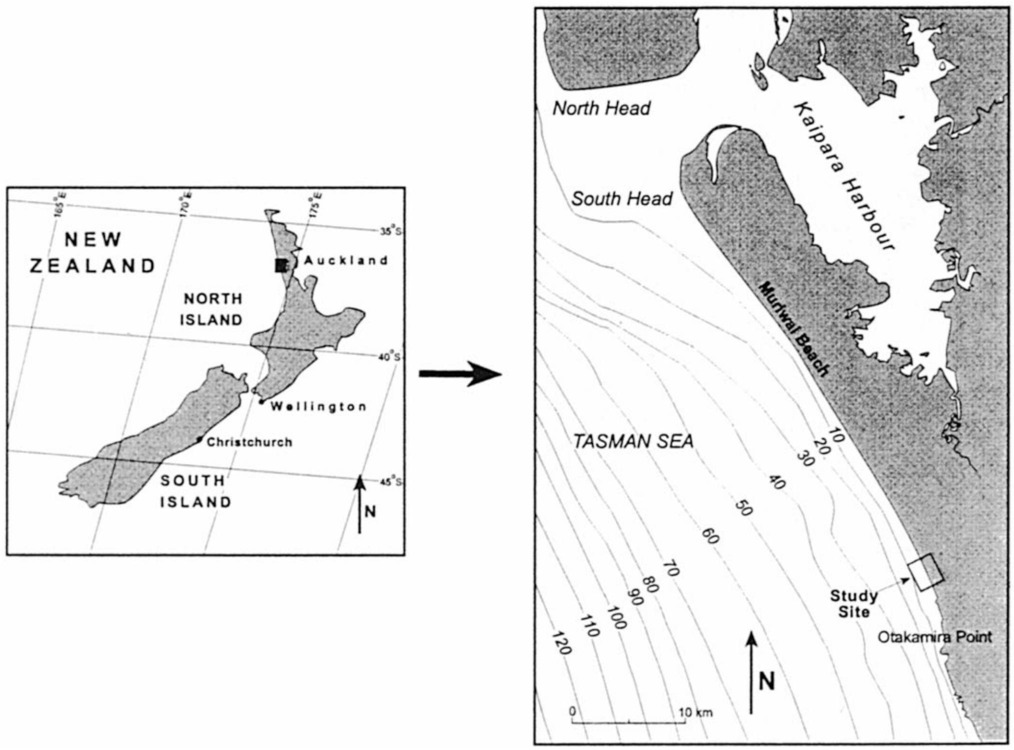

Fig. 1. Location of study site.

the offshore transport of water, sediments, pollutants and swimmers, rips remain a poorly understood phenomenon primarily due to the logistical difficulties involved in obtaining in situ field measurements. Although there has been a recent resurgence of field studies relating to rip currents (e.g. Aagaard et al., 1997; Symonds et al., 1997; Brander, 1999), these and previous studies (e.g. Sonu, 1972; Sasaki and Horikawa, 1975, 1978; Short, 1985; Kraus and Nakashima, 1987; Bowman et al. 1988a,b) have been limited to relatively low wave conditions. Virtually nothing is known about the role of rip currents on high-energy coasts, which is unfortunate since most beach systems are episodically driven by high-energy activity across the surf zone.

High-energy coasts are typical of storm-wave dominated and west coast swell environments (Davies, 1980), but no formal definition exists which delineates "high" from "low" energy conditions. Eliot (1973) used a breaking wave height (H_b) of 1.5 m to distinguish the two, while Short (1986) used thresholds of low- ($H_b < 1.5$ m), moderate- ($H_b =$ 1.5–2.5 m) and high-energy ($H_b > 2.5$ m), but no commonly accepted thresholds exist. Not surprisingly, field data from high-energy nearshore zones are rare (e.g. Wright et al., 1978, 1982; Beach and Sternberg, 1992; Davidson et al., 1993; Osborne and Rooker, 1999; Russell and Huntley, 1999), and direct quantitative measurements of rip currents in these environments are to date non-existent. This paper describes results obtained from a field experiment conducted in a rip current on a high-energy, west coast swell environment at Muriwai Beach, New Zealand. The site was chosen since its meso-tidal tide range provided an opportunity to deploy instrumentation at low tide. The aims of this paper are: (i) to examine the morphology and flow characteristics of a large-scale rip system; (ii) to assess the morphodynamic character and role of large-scale rips in a high-energy surf zone; and (iii) to investigate potential scaling relationships between these and lower-energy rip systems.

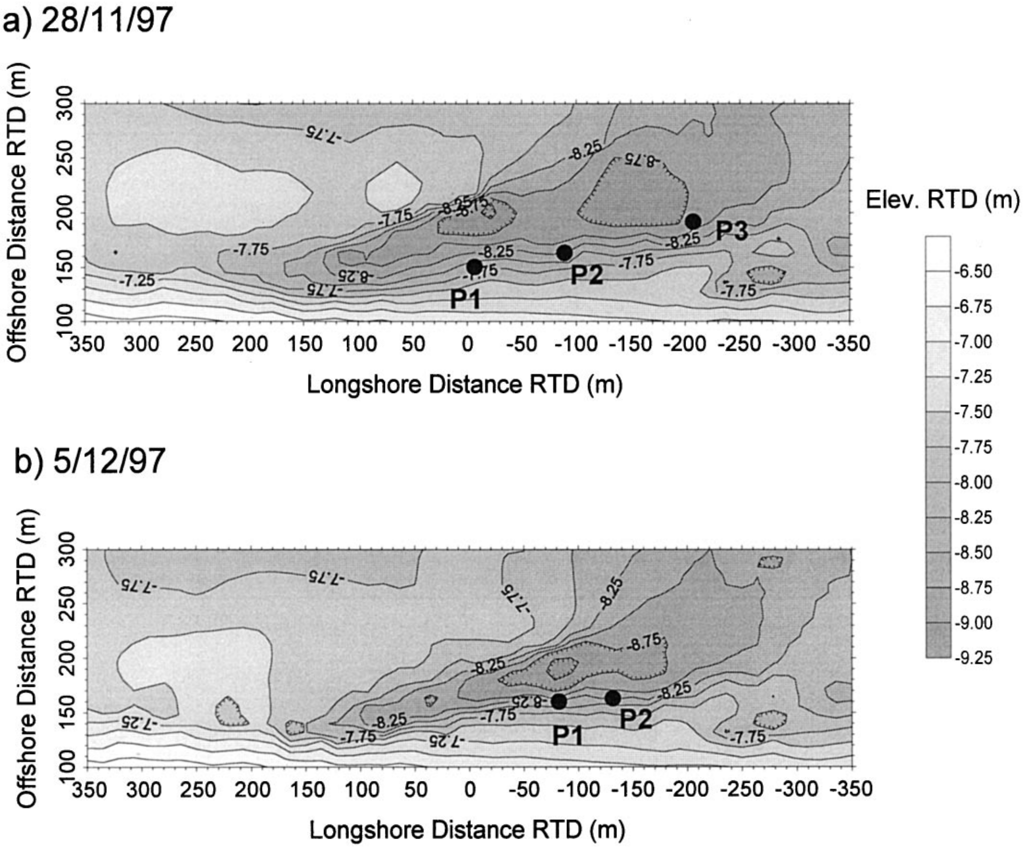

Fig. 2. Contour plots of the rip system for: (a) MUR1 (28/11/97); and (b) MUR2 (5/1/97) showing instrument pod (P1, P2, P3) locations. RTD = relative to datum.

2. Field site

Muriwai Beach is located on the west coast of New Zealand's North Island, approximately 35 km west of Auckland (Fig. 1), and lies at the southern end of an extensive Holocene Beach and dune barrier system extending 50 km north to the Kaipara Harbour. There has been a general trend of erosion along this beach over the past few decades and net sediment transport is generally considered to be northward. The experimental site was situated 3.5 km north of the southern end of the beach, and is completely exposed to the dominant south-westerly wind and swell regime. The beach is characterised by a mixed wave climate consisting of locally generated wind waves and swell from more remote storms in the Southern Ocean (Pickrill and Mitchell, 1979). Long-term wave climate information is unavailable for the site, but observations indicate incident swell periods of 10–15 s and breaking wave heights ranging from 2–5 m. The semi-diurnal tidal regime is meso-tidal and mean spring tide range is almost 4 m. The beach and surf zone sediments are composed of generally fine (<0.25 mm) material comprised principally of quartz and feldspar, but with significant rock and heavy mineral fractions (Schofield, 1970; Hamill and Balance, 1985). The nearshore is gently sloping with a gradient of 0.01. The surf zone is usually 400–500 m wide and consists of an inner bar exhibiting intermediate beach state topography and a more dissipative outer bar (Wright and Short, 1984). During high-energy storm events, the surf zone may exceed 800 m in width as more dissipative conditions dominate, particularly on the outer bar.

3. Methods

Data were collected on rip spacing, beach morphology and morphological change, nearshore water surface elevation and both eulerian and lagrangian feeder and rip flow. Measurements of longshore rip spacing along the entire beach length were obtained at both the beginning (27/11/97) and end (7/12/97) of the experiment by driving a 4WD vehicle along the upper beach face at low-tide and taking odometer readings at the position of every rip-neck. Nearshore morphology and topographic changes were surveyed directly using a total station and prism at the beginning of the experiment (28/11/97) with subsequent surveys coinciding with the instrument deployments (1/12/97 and 6/12/97). Surveys were conducted around low tide along 15 cross-shore transects centred around a primary zero line and separated by a longshore distance of 50 m, thereby encompassing a 700 m stretch of beach. Additional survey resolution was obtained by concentrating measurements along the banks of the feeder and rip channels. Due to safety constraints, the offshore extent of the surveys was restricted to the seaward slope of the first bar. In order to maximise the extent of surveys in the more dynamic inner surf zone the subaerial beach and upper intertidal zone were only surveyed on 28/11/97. This was deemed acceptable since topographic change in these areas during the experiment was negligible.

Water surface elevations and eulerian longshore and cross-shore current velocities were measured using strain gauge pressure sensors and bi-directional, ducted flowmeters mounted on weighted, portable pods designed for use in the energetic surf zone. The pods are buried up to their bases and their orientation is checked at the beginning and end of each experiment. Despite great strain placed on the instrument cables, the pods were not dislodged during the deployments. Three instrument stations, referred to as Pods 1–3 (P1–P3) were deployed on 1/12/97 (MUR1), whereas only two pods (P1 and P2) were deployed on the evening of 5/12/97 (MUR2). Due to logistic and safety constraints, it was only possible to deploy the pods at low tide and only on the landward margin of the feeder and rip channel (Fig. 2). Pressure sensors were mounted at an elevation (z) of 0.25 m above the bed. Flowmeters were mounted at $z = 0.6$ and 1.0 m for MUR1, whereas for MUR2 they were mounted at $z = 0.5$ and 0.9 m. Additional lagrangian information on the direction and velocity of rip flow were obtained using the rip float method described by Short and Hogan (1994), in which a person floating freely in the rip current is tracked by two theodolites recording positions every 30 s. A total of five rip floats were conducted on 30/11/97.

All sensors were hardwired to a shore-based mobile laboratory where the data was collected at a sampling frequency of 2 Hz for 34 min runs, each run separated by a minute. The data collection period began and ended around low tide on 1/12/97 with a total of 16 data runs obtained over a 9 h period. On 5/12/97 and 6/12/97, 22 data runs over a 12 h period were obtained encompassing a complete low–high–low tide cycle. Measurements of the breaking wave height (H_b) and wave period (T) in the outer surf zone were estimated visually. Readings from the pressure sensors were converted to water-surface elevation using Nielsen's (1989) method of local approximations. Flowmeter data were corrected for frequency-response characteristics using the techniques of Nielsen and Cowell (1981).

4. Morphological characteristics

Prior to the experiment, Muriwai Beach was subjected to a severe storm event with estimated breaking wave heights in excess of 3–4 m resulting in extensive beach erosion and scarping of the foredunes along the entire length of beach. With decreasing energy conditions ($H_b = 1.5$–2.5 m), the beach subsequently went through a period of rapid morphological readjustment. On 27/11/97 Muriwai exhibited strong longshore bar and trough morphology with extensive longshore feeder channels feeding into rip-neck channels oriented primarily to the northwest. The mean spacing of the 54 observed rips was 750 m ($\sigma = 389$ m). The single rip system monitored in this study was characterised by a 400 m long feeder channel fully contained in a pronounced trough between the inner bar and low-tide beachface. The width of the feeder increased from 50 m in the south to approximately 100 m in the north as it turned into an approximately 150 m wide rip-neck. Rip floats showed that the offshore extent of rip flow was approximately 300 m seaward of the confluence of the longshore feeder and rip-neck channels.

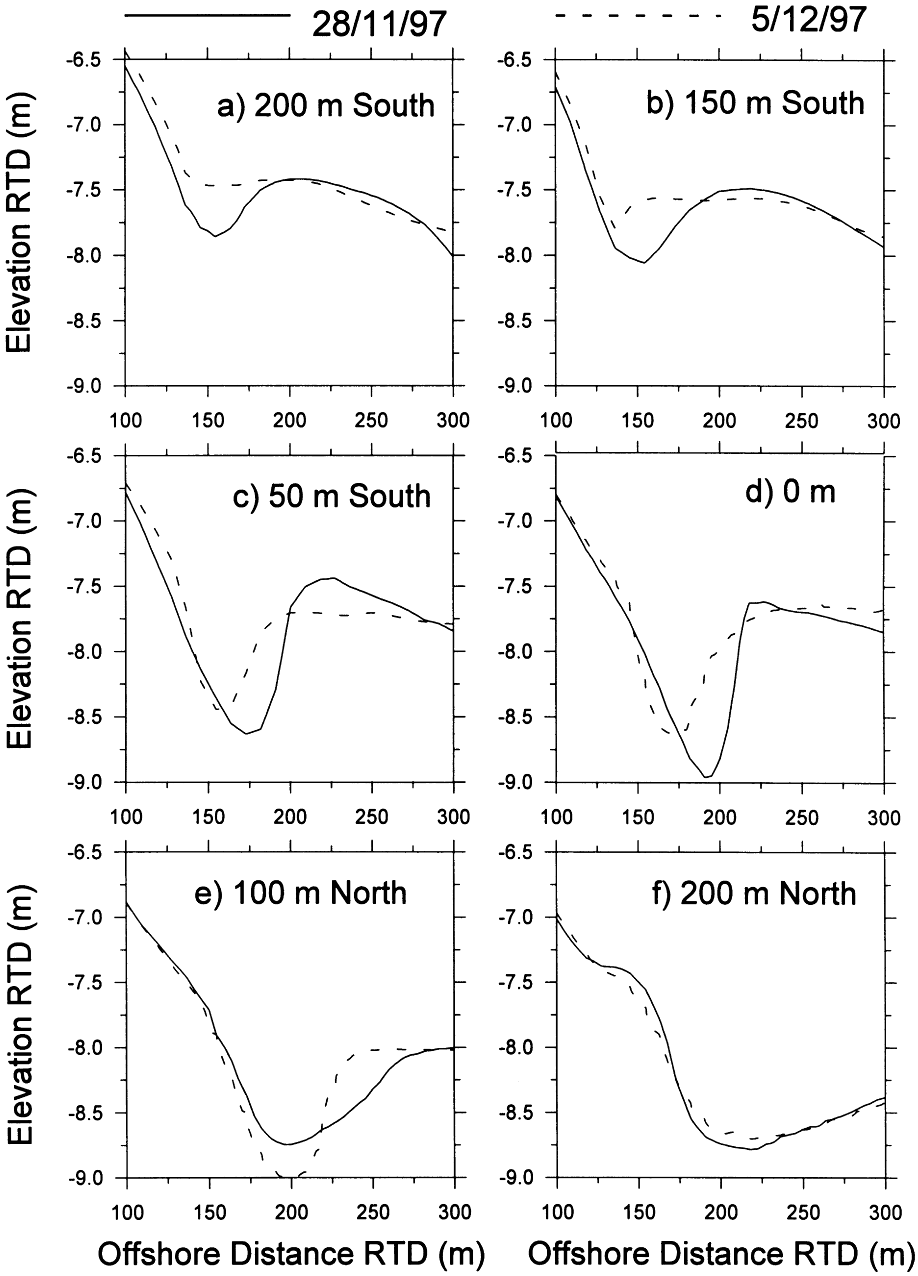

Fig. 3. Cross-sections of the longshore feeder and rip-neck channel illustrating bar migration and channel infilling between 28/11/97 and 5/12/97 for survey transects: (a) 200 m south; (b) 150 m south; (c) 50 m south; (d) 0 m north; (e) 100 m north; and (f) 200 m north.

By the end of the experiment, the morphological configuration of the beach and rip systems had changed significantly as the beach evolved towards a transverse bar and rip state. The number of rips along the beach on 7/12/97 ($n = 112$) had doubled and the average rip spacing of 365 m ($\sigma = 123$ m) was half that on 27/11/97 as the longshore bars migrated landward and welded to the beachface in

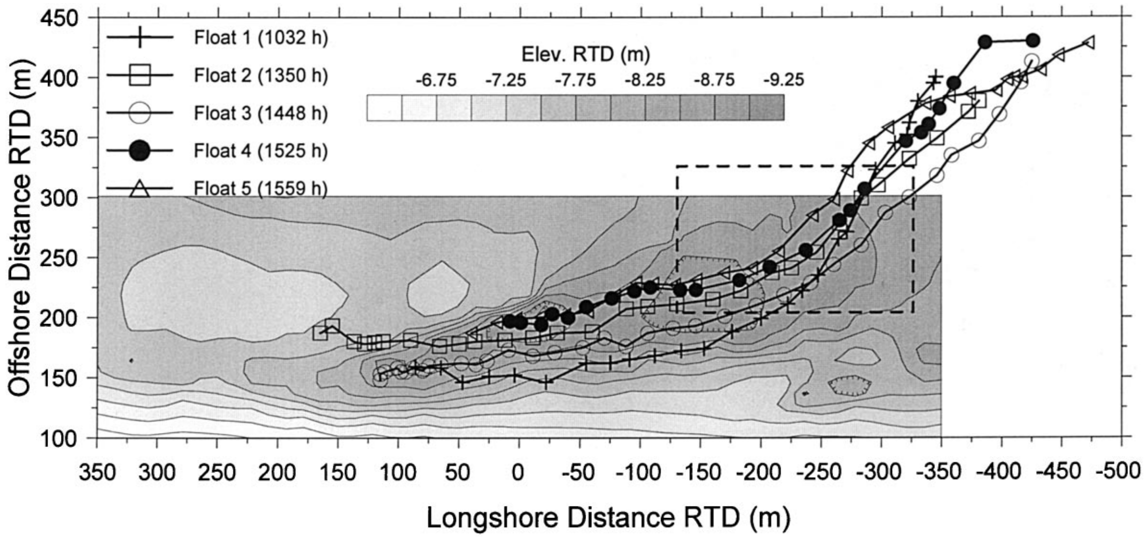

Fig. 4. Trajectories of the rip floats conducted on 30/11/97 with overlapping survey contour map of 28/11/97. Boxed region (dashed line) defines the region of maximum flow velocity. RTD = relative to datum.

many locations. This is apparent from the contour plot shown in Fig. 2b which indicates that the feeder channel experienced roughly 100 m of lateral infilling at the southern end, and was also approximately 30 m narrower in most places. A narrowing of the rip-neck channel was also observed in the field, largely due to a northern migration of the longshore bar, and this shift is apparent in Fig. 2b.

The cross-sections in Fig. 3 illustrate the patterns of bar migration more clearly. The position of the landward channel bank, which was defined by a pronounced beach step, migrated 5–10 m offshore at the southern end of the system (Fig. 3a–c), but migrated slightly landward near the rip-neck channel (Fig. 3d–f). The constriction and lateral infilling of the longshore feeder channel was clearly dominated by the landward migration of the inner bar which, as shown in Fig. 3, occurred along the entire length of the feeder. Bar migration rates for the period 28/11/97–6/12/97 varied from 2–6 m day^{-1} with maximums recorded at the southern end of the system, decreasing towards the rip-neck. As a result of this bar migration, the maximum morphological relief of the feeder channel ($y = 0$ m) decreased from approximately 1.6 to 1.2 m (Fig. 3d).

Table 1
Summary of lagrangian rip flow from rip floats conducted on 30/11/97. $\bar{u}_s$ = surface flow velocity over the entire rip flow trajectory; u_{smax} = maximum rip flow velocity recorded between two points

Float	Time (h)	Total $\bar{u}_s$ (m s^{-1})	u_{smax} (m s^{-1})	Cumulative distance (m)
1	1032	0.62	1.0	556
2	1350	0.69	1.15	594
3	1448	0.67	1.15	646
4	1525	0.73	1.25	495
5	1559	0.74	1.37	589

5. Lagrangian rip flow measurements

As shown in Fig. 4, lagrangian measurements of surface flow based on tracking of rip floaters extended from the start of the feeder channel, through the rip-neck and seaward to the rip-head over cumulative distances of up to 650 m (Table 1). The first float was initiated 2 h after high tide and the last ended 20 min before low tide on 30/11/97. In general, surface flow speeds were modulated by the tide. The mean surface flow velocity (u_s) of the rip, over the full float extent, increased from approximately 0.6 to 0.75 m s^{-1} (Table 1) and maximum mean flow velocities (u_{smax}), between points along the surface trajectory, increased from 1 to 1.4 m s^{-1} from high to low tide

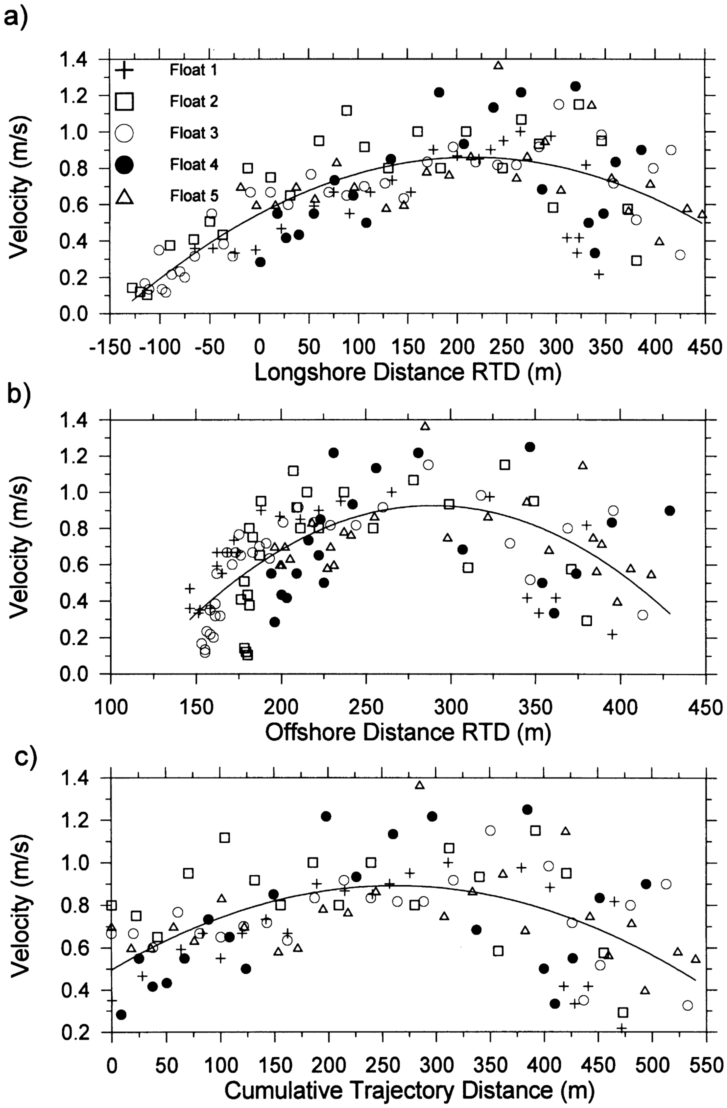

Fig. 5. Spatial patterns of rip float surface velocity showing variations: (a) in the longshore direction; (b) in the cross-shore direction; and (c) along the float trajectory. Fitted curves represent second-order polynomial functions.

(Table 1). It also appears that the surface trajectories of the floats shown in Fig. 4 tended to flow towards the deeper part of the channel as tide levels decreased. It should be noted that although the trajectories are influenced by the initial starting point, rip floaters were instructed to initiate the float in the strongest region of flow.

Distinct spatial patterns of surface flow velocity along the course of the rip were also evident. Fig. 5 shows all of the float velocity data in the longshore, cross-shore and trajectory directions and in all cases similar spatial trends are described by second-order polynomial functions. Flow velocity at the southern base of the feeder ($y = -150$ to -50 m) was relatively weak with speeds ranging from 0.1–0.4 m s^{-1}, but quickly increased in strength towards the north with velocities in the main body of the feeder ($y = -50$ to -100 m) on the order of

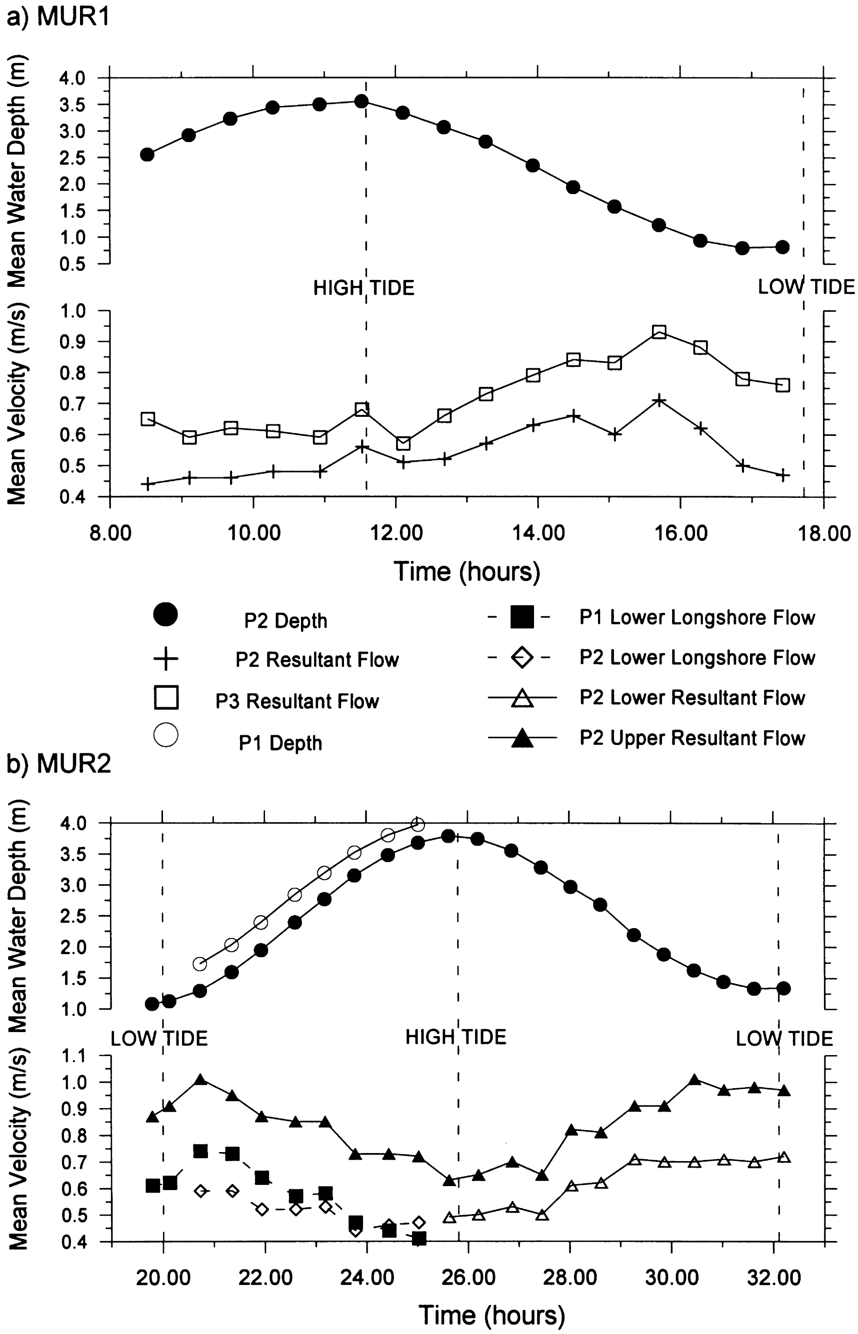

Fig. 6. Temporal variation in water depth and mean rip flow velocity for (a) MUR1; and (b) MUR2.

0.4–0.7 m s^{-1} (Fig. 5a). Flow maximums in the rip-neck ranged from approximately 0.8–1.2 m s^{-1} before decreasing again to <0.8 m s^{-1} in the rip-head (Fig. 5a and b). A similar velocity pattern was found along the rip trajectory, but in this case the velocity drop-off in the rip-head was more pronounced (Fig. 5c). Using an arbitrary cut-off velocity of 0.8 m s^{-1}, the polynomial fits in Fig. 5a and b define a region of maximum

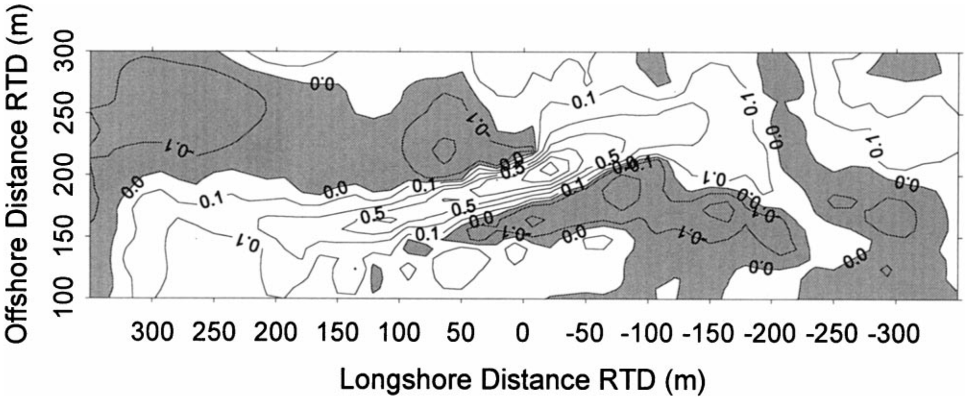

Fig. 7. Contour plot of net volumetric change between MUR1 and MUR2. Lighter shading represents areas of net deposition. Contours are in metres.

surface flow velocity within the rip, which is outlined by the dashed box in Fig. 4. This region includes the maximum lagrangian velocity measurements for each float and is situated at the feeder/rip-neck transition where the channel is deepest and the flow turns obliquely offshore. In summary, it appears that the strongest flows occur over the channel thalweg. This observation is consistent with the observations from low-energy rip systems reported by Brander (1997).

6. Eulerian rip flow measurements

Eulerian measurements of rip flow were restricted to the landward margin of the feeder and rip channel (Fig. 2), outside the region of maximum flow defined in Fig. 4. Wherever possible, resultant flow vectors ($\vec{u}_r$) were calculated, but due to instrument failure, this was not always possible. Early data records from 1/12/97 were hindered by gale-force winds from the north-west which produced a southerly flowing current in the swash zone that inhibited the northerly flow of the rip feeder and destroyed the cables to Pod 1. This southerly flow was a persistent factor throughout the deployment, but decreased in strength following a directional wind shift to the south-west at approximately 1000 h and an increase in water depth with the rising tide. Despite the dampening effects on rip flow from surface wind drift, resultant mean flow velocities ($\vec{u}_r$) at Pod 3 were on the order of 0.6 m s^{-1} and increased steadily with the falling tide, reaching a maximum of 0.93 m s^{-1} 2 h before the low tide (Fig. 6a). Maximum instantaneous velocities ($\vec{u}_{max}$) peaked at 1.8 m s^{-1}. MUR2 was not hindered by strong winds, and larger flows were recorded with $\vec{u}_r$ exceeding 1 m s^{-1} around successive low tides (Fig. 6b) and values of $\vec{u}_{max}$ reaching 2 m s^{-1}. These stronger flows are likely a reflection of the closer proximity of the MUR2 pods to the deeper channel and maximum flow region of rip flow (Fig. 2).

In general, flow velocities increased towards the rip-neck and also increased with elevation above the bed. Despite a longshore separation distance of only 20 m, values of $\vec{u}_r$ at Pod 3 during MUR1 were typically 0.2 m s^{-1} greater than those at Pod 2 (Fig. 6a). Similar spatial gradients in rip velocity have also been recorded in low-energy rip systems (Brander, 1997). Such spatial variation is not immediately apparent between Pods 1 and 2 during MUR2, but longshore flow velocities were certainly less at Pod 1 towards high tide (Fig. 6b). Unfortunately, information from Pod 1 ceased shortly before high tide when the cables to the instruments snapped. As shown in Fig. 6b, measurements of $\vec{u}_r$ at the upper sensor at Pod 2 were consistently stronger than at lower depths. Brander (1997) found that the strength of rip-neck flow increased away from the bed and then decreased towards the surface. Therefore, it is likely that $\vec{u}_r$, at depths in the fastest flowing portion of the rip-neck, was in excess of the lagrangian flows in this region, which varied from 1–1.4 m s^{-1}. This implies that mean flows on the order of 1.5 m s^{-1} likely occurred at low tide.

Recent studies (Aagaard et al., 1997; Brander, 1999) have shown that rip flow velocity is tidally modulated, with maximum flow speeds occurring around low tide and minimums near high tide. This modulation is also apparent at Muriwai Beach (Fig. 6). The offset timing of this modulation at low tide on 1/12/97 (Fig. 6a) can be attributed to both the enhanced effects of wind-driven surface drift and the locational shifting of the region of maximum flow (Fig. 4). In both deployments, the difference in mean flow strength between low and high tides is approximately $0.4\ \mathrm{m\ s^{-1}}$. Also of interest is the temporal symmetry of flow strength observed during MUR2 with $\vec{u}_r$ being identical at $1\ \mathrm{m\ s^{-1}}$ for both low tides.

7. Sediment transport

Direct measurements of sediment transport were not made in the rip system, but it is possible to make some inferences based on profile adjustments. Fig. 7 is a contour plot of net sediment volume changes in the rip survey grid between 28/11/97 and 5/12/97. Despite the problems involved in surveying some of these areas, particularly the rip-neck, and inherent limitations of the contouring program, several patterns are evident. First, net accretion was dominant near the feeder channel, which experienced up to 1 m of infilling in places. Second, net erosion on the order of 0.2 m over a large extent of the longshore bar is evident and there is some evidence to suggest that erosion at the base of the rip-neck occurred. Gross estimates of volumetric sediment adjustment suggest that infilling rates for the entire length of the feeder channel were on the order of $550\ \mathrm{m^3\ day^{-1}}$.

8. Discussion

At present, there exists a paucity of flow velocity measurements made in rip current environments. Those reported tend to vary due to the use of different measurement techniques such as drogues (e.g. Shepard and Inman, 1950; Sasaki and Horikawa, 1975, 1978), dye (e.g. Talbot and Bate, 1987; Huntley et al., 1988) and various types of flowmeters (e.g. Sonu, 1972; Bowman et al., 1988a,b; Sherman et al. 1993; Smith and Largier, 1995; Aagaard et al., 1997; Brander, 1999). In addition, rip measurements are hindered by locational variation within the rip/feeder channel and variety in rip system types. In general, the studies mentioned above were conducted in relatively low-energy environments where H_b ranged from 0.5–1.5 m and mean and maximum instantaneous rip flow velocities were on the order of $0.2–0.6\ \mathrm{m\ s^{-1}}$ and $0.8–1.2\ \mathrm{m\ s^{-1}}$, respectively. In contrast, measurements in this study were obtained in surf zones where H_b was on the order of 2–2.5 m, $\bar{u}_r$ on the edge of the rip channel reached $1\ \mathrm{m\ s^{-1}}$, and maximum instantaneous velocities commonly exceeded $2\ \mathrm{m\ s^{-1}}$. These data are unique in the literature and possibly represent the strongest rip current flows measured to date. However, to be placed in a morphodynamic perspective, the nature and type of rip current system that exists at Muriwai should be examined in further detail.

Short (1985) classified rips into three basic types: (i) accretion rips which occur under decreasing energy conditions; (ii) erosion rips which occur under increasing energy conditions; and (iii) mega-rips which are topographically controlled erosion rips that persist under high-energy conditions ($H_b >$ 3 m). Muriwai Beach has a dissipative outer surf zone and an intermediate inner bar system, as is commonly observed on multi-bar systems (Short and Aagaard, 1993). The morphodynamic conditions observed during this study and ongoing video imaging of the site (Donohoe, 1998) show that the inner surf zone typically remains intermediate, with widely spaced rips even during high wave conditions (outer bar ($H_b > 5$ m). During subsequent decreasing wave conditions, the inner bar evolves through the intermediate beach state sequence described by Wright and Short (1984) for single-bar systems. These observations indicate that even on high-energy exposed beaches with a dissipative outer surf zone, the inner surf zone evolves through the same bar–rip sequences of lower energy systems, though with much larger scale bar and rip dimensions, and higher current flow velocities. Despite the size (and velocity) of the rips observed during this experiment, it would be a misnomer to refer to them as erosion or mega-rips simply because of their scale and existence in a high-energy surf zone. They are simply large-scale accretion rips, as verified by the changes in beach morphology.

Table 2
Scaling comparison of low- and high-energy rip current systems using morphologic and hydyrodynamic parameters. H_b = breaking wave height; $\bar{u}_r$ = mean rip flow velocity; u_{max} = maximum instantaneous rip flow velocity; x_s = surf zone width

Parameter	Palm Beach (ECS)	Muriwai (WCS)	Scaling factor
Morphology			
Rip spacing (m)	200	500	2.5
Feeder length (m)	150	400	2.7
Feeder width (m)	20–40	50–100	2.5
Feeder relief (m)	0.6	1.4	2.3
Rip-neck length (m)	100	300	3
Rip-neck width (m)	60	150	2.5
Bar migration (m day^{-1})	3	4	1.3
Hydrodynamics			
H_b (m)	0.75	2	2.7
$\bar{u}_r$(m s^{-1})	0.4–0.6	1–1.5	2.5
u_{max} (m s^{-1})	2	2	1
x_s (m)	120–150	400–500	3.3

Using a comprehensive database of rip spacing and surf zone width on intermediate beaches encompassing a variety of regional wave climates, Short and Brander (1999) found that high-energy west coast swell environments, such as Muriwai, typically have rip spacings and surf zone widths which are 2.5 times greater than those on lower energy east coast swell environments. The existence of this scaling relationship was linked to variations in wave power (Short and Brander, 1999). The morphologic evolution observed during this experiment is virtually identical in nature to a recent sequence of intermediate beach state adjustment described by Brander (1999) on an east coast swell environment at Palm Beach, NSW, Australia. A comparison of the two datasets provides an excellent opportunity to examine the validity of this scaling relationship.

Both experiments were characterised by rapid bar migration and feeder infilling as the beaches tended towards a transverse bar and rip state. Similarly, both experiments found an increase in rip current flow velocity as the morphologic evolution progressed and active incision of the rip-neck channel as the feeders infilled. Table 2 provides a gross comparison of both morphologic and hydrodynamic parameters of the measured nearshore and rip systems. It is difficult to base conclusions on relationships between only two sets of data. However, the nature and quality of these datasets are rare and difficult to obtain. The comparisons are therefore useful, but have been simplified as much as possible to take into account the restricted dataset. The values for Palm Beach are given as averages and/or ranges for similar stages of beach state evolution. The values have not been non-dimensionalised and, in the case of Muriwai, H_b and surf zone width (x_s) are based on visual estimations (Table 2).

Despite these limitations, the scaling relationships shown in Table 2 are similar to that found by Short and Brander (1999) for west and east coast swell intermediate beaches. In terms of morphology, the length and width of rip feeder and neck channels at Muriwai were all very close to being 2.5 times greater than those at Palm Beach. The major discrepancy is rip-neck length, but the values for this parameter are based on approximations since survey resolution in this region is poor. Mean bar migration rates were similar, but it is difficult to assess this parameter since rates varied considerably in the longshore direction and reported bar migration rates in the literature have traditionally been quite variable (Sunamura and Takeda, 1984). More significant is the scaling relationship observed for the measured ranges of mean rip flow velocity ($\bar{u}_r$) during the experiments (Table 2). Flows at Muriwai were exactly 2.5 times greater than at Palm Beach. Instantaneous rip flow velocities were similar at approximately 2 m s^{-1}, but this is not surprising since both rip systems were observed to exhibit pulsatory behaviour.

The existence of such a scaling factor implies that the physical connection between waves, currents and morphology, both within and between beach systems, are related to variations in wave energy. Specifically, these energy levels must in some way influence longshore variations in radiation stress gradients (Bowen, 1969; Bowen and Inman, 1969), mass transport and flow discharge relationships, and hence sediment transport patterns within the surf zone. Unfortunately, it is not possible to provide a rigorous analysis of these phenomena from the data obtained in this study. However, the fundamental criterion for the scaling factor was based on observations of rip spacing (Short and Brander, 1999), and previous studies by Hino (1974) and Huntley and Short (1992) have shown that rip spacing is theoretically scaled with surf zone width. As wave height and surf zone width increase so too does rip spacing. Nevertheless, no theory yet exists which has consistently and successfully applied existing models of rip generation and rip spacing to the observed patterns of rip current form and process. This study provides additional evidence for scaling relationships between rip current systems, but acknowledges that explanations for the physical mechanisms of these relationships remain to be resolved.

9. Summary and conclusions

The results presented in this paper have provided some valuable insights into rip current behaviour in high-energy surf zones. First, quantitative measurements have been achieved which, for the first time, give an idea of the magnitude of both rip system morphology and kinematic parameters in this environment. Second, rip currents on high-energy beaches characterised by intermediate beach state morphology and decreasing energy conditions behave almost identically to their counterparts on low-energy beaches and are best described as large-scale accretion rips. Third, there is evidence to suggest that distinct scaling relationships exist between intermediate beaches on west coast and east coast swell environments. Ongoing research on these relationships is clearly necessary, but the apparent scaling of nearshore morphological and hydrodynamic variables may be useful in the prediction of rip dimensions and dynamics as well as future modelling of rip current and intermediate beach state behaviour.

Acknowledgements

This project was funded by an Australian Research Council Collaborative Grant to A.D.S. We are indebted to Michael Hughes (Sydney), Dave “I’ve got some good news and some bad news” Mitchell (senior technical officer, Sydney) and Phil Osborne (Auckland) for their excellent help in the field and for comments on early versions of this manuscript. Paul Villard, Dave Jenkinson and Shane Thomson are also thanked for helping us in the field. The rip floats could not have been attempted without the assistance of the Muriwai Beach Surf Life Saving Club who not only rescued the rip floaters, but volunteered for some themselves. Thanks also to Anne Mason for securing us accommodation and to Dave Jackman for keeping it tidy.

References

Aagaard, T., Greenwood, B., Nielsen, J., 1997. Mean currents and sediment transport in a rip channel. Mar. Geol. 140, 25–45.

Beach, R.W., Sternberg, R.W., 1992. Infragravity driven suspended sediment transport in the swash, inner and outer surf zone. Proceedings of Coastal Sediments ‘91, pp. 114–128.

Bowen, A.J., 1969. Rip currents. Part 1. Theoretical investigations. J. Geophys. Res. 74 (23), 5467–5478.

Bowen, A.J., Inman, D.L., 1969. Rip currents. Part 2. Laboratory and field observations. J. Geophys. Res. 74 (23), 5479–5490.

Bowman, D., Rosen, D.S., Kit, E., Arad, D., Slavicz, A., 1988. Flow characteristics at the rip current neck under low energy conditions. Mar. Geol. 79, 41–54.

Bowman, D., Arad, D., Rosen, D.S., Kit, E., Goldbery, R., Slavicz, A., 1988. Flow characteristics along the rip current system under low-energy conditions. Mar. Geol. 82, 149–167.

Brander, R.W., 1997. Field observations on the morphodynamics of rip currents. PhD thesis, Department of Geography, University of Sydney. (240pp., unpublished).

Brander, R.W., 1999. Field observations on the morphodynamic evolution of a low-energy rip current system. Mar. Geol. 157, 199–217.

Davidson, M.A., Russell, P.E., Huntley, D.A., Cramp, A., Hardisty, J., 1993. An overview of the British Beach and Nearshore Dynamics (B-BAND) programme. Proceedings of the 23rd International Conference on Coastal Engineering, ASCE, pp. 1987–2000.

Davies, J.L., 1980. Geographical Variation in Coastal Development, Longman, London (212pp.).
Donohoe, B.F.P., 1998. Spatial and temporal bar morphodynamics of Muriwai Beach. MSc thesis, Department of Geography, University of Auckland. (104pp., unpublished).
Eliot, I., 1973. The persistence of rip current patterns on sandy beaches. Proceedings of the First Australian Conference on Coastal Engineering, pp. 29–34.
Hamill, P.F., Balance, P.F., 1985. Heavy mineral rich beach sands of the Waitakere coast, Auckland, New Zealand. N.Z. J. Geol. Geophys. 28, 503–511.
Hino, M., 1974. Theory on formation of rip current and cuspidal coast. Proceedings of the 14th Conference on Coastal Engineering, pp. 901–919.
Huntley, D.A., Short, A.D., 1992. On the spacing between observed rip currents. Coast. Engng 17, 211–225.
Huntley, D.A., Hendry, M.D., Haines, J., Greenidge, B., 1988. Waves and rip currents on a Caribbean pocket beach. Jamaican J. Coast. Res. 4 (1), 69–79.
Kraus, N.C., Nakashima, L., 1987. Field measurement in a rip current: fluid and sediment movement. EOS 68, 1311–1312.
Lippman, T.C., Holman, R.A., 1990. The spatial and temporal variability of sand bar morphology. J. Geophys. Res. 95, 11575–11590.
Nielsen, P., 1989. Analysis of natural waves by local approximations. J. Waterway Port Coast. Ocean Engng 115, 384–396.
Nielsen, P., Cowell, P.J., 1981. Calibration and data correction procedures for flow meters and pressure transducers commonly used by the Coastal Studies Unit. Coastal Studies Unit, University of Sydney Technical Report 81/1 (33pp.).
Osborne, P.D., Rooker, G.A., 1999. Sand re-suspension under high energy infragravity swash Bethells beach, New Zealand. J. Coast. Res. 15 (1), 74–86.
Pickrill, R.A., Mitchell, J.S., 1979. Ocean wave characteristics around New Zealand. NZ J. Mar. Freshw. Res. 13 (4), 501–520.
Russell, P.E., Huntley, D.A., 1999. A cross-shore transport “shape function” for high energy beaches. J. Coast. Res. 15 (1), 198–205.
Sasaki, T., Horikawa, T., 1975. Nearshore current system on a gently sloping bottom. Coast. Engng Jpn. 18, 123–142.
Sasaki, T., Horikawa, K., 1978. Observation of nearshore current and edge waves. Proceedings of the 16th Conference on Coastal Engineering, pp. 791–809.
Schofield, J.C., 1970. Coastal sands of Northland and Auckland. NZ J. Geol. Geophys. 13, 767–824.
Shepard, F.P., Inman, D.L., 1950. Nearshore circulation related to bottom topography and wave refraction. Trans. Am. Geophys. Union 31 (4), 555–565.
Sherman, D.J., Short, A.D., Takeda, I., 1993. Sediment mixing-depth and bedform migration in rip channels. J. Coast. Res. 15, 39–48 (special issue).
Short, A.D., 1985. Rip current type, spacing and persistence, Narrabeen beach, Australia. Mar. Geol. 65, 47–71.
Short, A.D., 1986. A note on the controls of beach state and change, with examples from south-east Australia. J. Coast. Res. 3 (3), 387–395.
Short, A.D., Aagaard, T., 1993. Single and multi-bar beach change models. J. Coast. Res. 15, 141–157 (special issue).
Short, A.D., Brander, R.W., 1999. Regional variations in rip density. J. Coast. Res. 15 (3), 813–822.
Short, A.D., Hogan, C.L., 1994. Rip currents and beach hazards: their impact on public safety and implications for coastal management. J. Coast. Res. 12, 197–209 (special issue).
Smith, J.A., Largier, J.L., 1995. Observations of nearshore circulation: rip currents. J. Geophys. Res. 100 (C6), 10 967–10 975.
Sonu, C.J., 1972. Field observation on nearshore circulation and meandering currents. J. Geophys. Res. 77, 3232–3247.
Sunamura, T., Takeda, I., 1984. Landward migration of inner bars. Mar. Geol. 60, 63–78.
Symonds, G., Holman, R.A., Bruno, B., 1997. Rip currents. Proceedings of Coastal Dynamics ‘97, ACSE, pp. 584–593.
Talbot, M.M.B., Bate, G.C., 1987. Rip current characteristics and their role in the exchange of water and surf diatoms between the surf zone and nearshore. Estuar. Coast. Shelf Sci. 25, 707–720.
Wright, L.D., Short, A.D., 1984. Morphodynamic variability of surf zones and beaches: a synthesis. Mar. Geol. 56, 93–118.
Wright, L.D., Thom, B.G., Chappell, J., 1978. Morphodynamic variability of high-energy beaches. Proceedings of the 16th Conference on Coastal Engineering, pp. 1180–1195.
Wright, L.D., Chappell, J., Thom, B.G., Bradshaw, M.P., Cowell, P., 1979. Morphodynamics of reflective and dissipative beach and inshore systems: southeastern Australia. Mar. Geol. 32, 105–140.
Wright, L.D., Guza, R.T., Short, A.D., 1982. Dynamics of a high-energy dissipative surf zone. Mar. Geol. 45, 41–62.